Title:
Cell-cycle dependent transcription, a determinant factor of heterogeneity in cationic lipid-mediated transgene expression

Running Title:
Mechanism of heterogeneity in lipoplex

Author affiliation:
Hidetaka Akita[1,2], Rie Ito[1,2], Hiroyuki Kamiya[1,2], Kentaro Kogure[1,2] and Hideyoshi Harashima[1,2,*]

[1]Graduate School of Pharmaceutical Sciences, Hokkaido University, Sapporo, Hokkaido 060-0812, Japan

[2]CREST, Japan Science and Technology Agency (JST), Japan

Corresponding author:
Hideyoshi Harashima, Graduate School of Pharmaceutical Sciences, Hokkaido University, Sapporo, Hokkaido, 060-0812, Japan.
Telephone: +81-11-706-3919
Fax: +81-11-706-4879
E-mail: harasima@pharm.hokudai.ac.jp

Key Words: heterogeneity, nuclear delivery, transcription, non-viral, gene transfer, HeLa

Abstract

Background

Heterogeneity of transgene expression, the presence or absence (below the limit of detection) of transgene expression on a cell-by cell basis, is a severe disadvantage in the use of cationic lipid-mediated gene vectors for gene therapy and experiments in molecular biology. Understandings of intracellular trafficking and the function (transgene expression) of vectors related to cellular physiology are essential in terms of clarifying the mechanism underlying the heterogeneity.

Methods

To distinguish the contribution of nuclear transfer efficiency and subsequent intranuclear transcription efficiency to the overall heterogeneity in transgene expression, a novel imaging system was established for the dual visualization of the nuclear transfer of pDNA and marker gene expression (lacZ) in single cell.

Results

The expression of LacZ occurred in only approximately 30% of HeLa cells of the nuclear pDNA-positive cells, indicating that intranuclear transcription efficiency contributed to the heterogeneity. Dual imaging against synchronized cells further revealed that the efficiency of nuclear delivery was comparable irrespective of cell cycle status, which is contrary to the generally accepted hypothesis that nuclear import of pDNA is enhanced during cell division when the nuclear membrane structure is perturbed. The most significant finding in the present study is that nuclear transcription efficiency in terms of the ratio of LacZ-positive cells to nuclear pDNA-positive cells drastically increased in the late S and G2/M phase.

Conclusion

This is the first demonstration to show that cell cycle-dependent intranuclear transcription appears to be responsible for the overall heterogeneity of transgene expression.

Introduction

Non-viral gene vectors, such as cationic liposomes are highly potent and promising devices for safe gene therapy. However, their application has been restricted because of their low transfection activity, compared with viral vectors. One of the reasons for this low transfection efficiency includes the heterogeneity of the transgene expression, the presence or absence (below the limit of detection) of transgene expression on a cell-by cell basis. Despite various efforts to improve it, the percentage of transgene expression-positive cells is limited to less than 30-50%[1, 2], whereas, for the adenoviral vector, this value generally exceeds 80%[3, 4].

To understand the mechanism of the heterogeneity completely, adequate experimental systems need to be developed. A cell lysate-based measurement of transgene expression such as the luciferase assay is not adequate, since it cannot extract information concerning transgene expression in an individual cell[5-8]. Flow cytometry analyses provide important information on the heterogeneity of transgene expression[9]. In fact, this technique revealed that the percent of marker gene expression-positive cells to all cells analyzed was sharply enhanced when the cells cycle progressed through the M phase[9], suggesting that heterogeneous transgene expression is derived from variations in the cell cycle status in a population of cells. However, even using flow cytometry, the measurement of transgene expression alone is not sufficient to permit the mechanism for the M-phase specific enhancement of transgene expression to be determined. Many investigators believe that the M-phase specific enhancement in transgene expression is due to the temporal breakdown of the nuclear membrane, which allow pDNA to access the nucleoplasm[5, 6, 10, 8, 9]. Less heterogeneous transgene expression in adenoviral vectors[3, 4], in which the system for the nuclear delivery of their genome is sophisticated

even in non-dividing cells[11-13], supports this general conclusion. However, very little direct evidence for improved nuclear delivery at the M-phase is available. In the present study, we first evaluate the intracellular trafficking (e.g. cellular uptake, endosomal escape and nuclear transfer) of lipoplex quantified by a recently developed confocal image-assisted 3-dimensionally integrated quantification (CIDIQ) method[14], which provides information concerning intracellular distribution of exogenous DNA in endosome/lysosome, cytosol and nucleus simultaneously in individual cell. A previous CIDIQ analysis permitted us to recognize that pDNA transfected by LFN was taken up by >95% of cells [14]. In contrast, the nuclear delivery of pDNA was only detected in less than 30% of the cells. It thus appears that the variation in nuclear transfer efficiency on a cell-to-cell basis is one of the determinants for heterogeneous transgene expression.

Furthermore, recent progress in epigenetics have revealed that intra-nuclear transcription is also dynamically regulated by the acetylation/methylation of histones[15, 16], methylation of DNA *per se* via the CpG motif[17, 18] and chromosome organization[19-21]. Indeed, transgene expression efficiency per one copy of exogenous DNA is rapidly altered in the nucleus after transfection [22, 23]. Therefore, it is highly possible that the pharmacodynamics (i.e. transcription) may also contribute to heterogeneous expression.

In the present study, we established a dual imaging system for the nuclear delivery of pDNA and transgene expression in individual cells, which enabled us to determine the transcription efficiency, which is defined as transgene expression-positive cells divided by nuclear pDNA-positive cells. Therefore, this novel method enables us the contribution of intranuclear transcription process to the overall heterogeneity of transgene expression to be determined.

Materials and Methods

Materials

LacZ-encoding pcDNA3.1 (pcDNA3.1-LacZ) and LipofectAMINE PLUS (LFN) were from Invitrogen Corp. (Carlsbad, CA, USA). Hoechst 33342 and propidium iodide (PI) was obtained from Wako Chemical (Osaka, Japan). In vivo lacZ β-Galactosidase Detection Kit (Product M0259) were purchased from Marker Gene Technologies Inc. (Eugene, OR, USA). Label IT reagent for labeling pDNA with rhodamine was from the Panvera Corporation, (Madison, WI, USA). HeLa cells were obtained from the American Type Culture Collection (Manassas, VA, USA). Other chemicals used were commercially available and were reagent grade products.

Cell synchronization

To synchronize HeLa cells in the G1 status, Cells were seeded at a density of 100,000 cells per 6-well plate in growth media. After 24 hour, the cells were incubated with 2 ml of hydroxyurea, reconstituted in growth media at a concentration of 2 mg/ml for 18 hour. Cell cycle-arrest was released by replacing the hydroxyurea-including media to hydroxyurea-free media. The synchrony persisted until the next G1 phase, which occurs, at the latest, 24 hour after release from the cell cycle-arrest.

Assessment of cell cycle status

At the indicated times after release from G1-arrest, the cell cycle status was assessed by flowcytometry measurements of permeabilized cells that had been stained with PI as described previously [24]. Before harvesting, cells were washed twice with 2 ml of PBS. The cells were then treated with 500 µl of 0.25% Trypsin/0.02% EDTA at 37^{o}C until they were completely detached from the plate. Trypsin was inactivated by the addition of an equal volume of cold growth media, and cells were isolated by centrifugation at 280 g for

5 min. Cells were washed two times by suspending them in 1 ml of PBS and were then isolated by centrifugation at 280 g for 5 min. Final cell precipitates were completely suspended in 300 µl of PBS. The cells were fixed with ethanol by applying 700 µl of cold 100% ethanol dropwise to the cell suspension during vortexing. After an overnight incubation at -20 ^{o}C, samples were centrifuged at 10,000 g for 5 min. The resulting cell pellet was suspended in 500 µl of cold PBS, and then incubated with 20 µg/ml of RNase I and 25 µg/ml of PI for 45 min at 37 ^{o}C in the dark. After filtration through a nylon mesh, 10,000 cells were analyzed in the FL-A channel (emission: 610 nm) of flow cytometer (FACScan, Beckton Dickinson, San Jose, CA, USA) with an Ar-ion laser (excitation: 488 nm). The pulse area (FL2-A) was plotted against pluse width (FL2-W) in individual cells, and then G_0/S doublets, which are clearly discriminated by large FL2-W, were then excluded from the analysis as demonstrated previously [25].

Dual imaging of nuclear delivery of pDNA and LacZ expression in individual cell

For the dual imaging of the intracellular distribution pDNA and LacZ expression in an individual cell, a 1:1 mixture of LacZ-encoding pDNA, along with that labeled with rhodamine by means of LabelIT reagent was transfected to HeLa cells by LFN following the manufacture's instruction. Briefly, HeLa cells were seeded at a density of 5 x 10^4 cells on a poly-D-lysine cell ware 35mm Glass Base Dish (IWAKI, Tokyo, Japan) 24 h before transfection. 2 µg of plasmid DNA and 12 µl of Plus reagent were incubated in 200 µl of serum free D-MEM for 15 min at room temperature, and mixed with the serum free D-MEM with 8 µl of LipofectAMINE, followed by further incubation at room temperature for 15 min. This solution was then transferred to 1 ml of serum-free cell D-MEM. After incubation for a total of 3 hour, the nucleus was stained by treatment with Hoechst 33342 for 10 min at a final concentration of 25 µM.

Transgene expression was further visualized using an in vivo lacZ β-Galactosidase Detection Kit with a minor modification in the recommended protocol. A 100 μl aliquot of fluorescein di-β-D-galactopyranoside substrate (10 mM) was diluted 10-fold with serum free DMEM (final concentration 1 mM), and incubated at 37^{o}C for 10 min in the dark. After washing the cells with 500 μl of PBS, the cells were incubated with the substrate solution at 37^{o}C for 15 min in the dark. For inactivation of the staining process, 1.8 ml of ice-cold DMEM including 4% FBS was applied to the cell culture.

When dual imaging was applied to the synchronized cells, HeLa cells were seeded at a density of 2.5 x 10^5 cells on a glass bottom dish 24 hour prior to synchronization. After synchronization to the G1 status by hydroxyurea treatment, as described above, cell cycle arrest was then terminated by replacing the media with hydroxyurea-free media.

Fluorescence image acquisition and data analysis

Fluorescence signals for the rhodamine (excitation: 543 nm, emission: 582 nm) and activated fluorescein di-β-D-galactopyranoside substrate catalyzed by LacZ (excitation: 488 nm, emission: 512 nm) along with bright field images were captured using a Zeiss Axiovert 200 inverted fluorescence microscope equipped with a 63 x NA 1.4 Planachromat objective (Carl Zeiss Co. Ltd.; Jena, Germany). After sequential 20 Z-series of images were captured for each cell, each 8-bit TIFF image was transferred to an Image-Pro Plus ver 4.0 (Media Cybernetics Inc., Silver Spring, MD) to quantify the brightness and pixel area of each region of interest.

Cellular uptake and the nuclear delivery of pDNA was quantified by confocal image-assisted 3-dimensionally integrated quantification (CIDIQ)[14]. For data analysis, the pixel areas of each cluster in nucleus; s_i (nuc) and other intracellular region: s_i (ext) were separately summed for each XY-plane, and are denoted as $S'_{Z=j}$(nuc), and $S'_{Z=j}$(ext),

respectively. The values of $S'_{Z=j}$(nuc) and $S'_{Z=j}$(ext) in each XY plane were further summed and are denoted as S(nuc) and S(ext), respectively. Furthermore, the total area of the pDNA, denoted as S(tot), was calculated by integrating the S(nuc) and S(ext).

To quantify the relative gene expression of LacZ, the middle xy-image (Z=10) of the Z-series images was extracted. Activated fluorescein di-β-D-galactopyranoside substrate was equally distributed in the whole cell. Then, the average fluorescence intensity per pixel was calculated as an index of gene expression. Control HeLa cells, excited at 488 nm were auto-fluorescent. The threshold intensity, above which the cells were defined as lacZ-positive cells were then determined. As a control, luciferase-encoding pDNA (pcDNA3.1-luc) was transfected and treated with phenylethyl β-D-thiogalactoside substrate. In these cells, the mean fluorescence intensity per pixel never exceeded 200 in all of the cells analyzed. In contrast, when pcDNA3.1-LacZ was transfected, 18 cells out of 100 cells analyzed clearly showed a strong fluorescence (mean intensity >200). The histogram of the mean fluorescence intensity per pixel for other cells was quite similar to that for control cells. Collectively, the threshold intensity to discriminate lacZ-expressing cells is defined as 200, in this study.

Luciferase assay

To establish stably transfected HeLa cells expressing CMV-driven luciferase, luciferase (GL3)-encoding pcDNA3.1 was transfected into HeLa cells by LFN and selected by treatment with 800 μg/ml of geneticin (G418) for two weeks as described previously [26]. Luciferase-positive cell population was maintained in the growth media with 400 μg/ml of G418.

At the indicated times after G1-arrest was released, the cells were washed, and were solubilized with reporter lysis buffer (Promega, Madison, WI). Luciferase activity was

initiated by the addition of 100 µl of luciferase assay reagent (Promega) to 20 µl of cell lysate, and the activity measured by means of a luminometer (Luminescencer-PSN, ATTO, Japan). The amount of protein in the cell lysate was determined using a BCA protein assay kit (PIERCE, Rockford, IL).

Results

Dual imaging of nuclear delivery of pDNA and transgene expression

Transgene expression is the result of multiple processes related to intracellular pharmacokinetics (i.e. cellular uptake, endosomal escape and nuclear delivery) and intranuclear pharmacodynamics (i.e. transcription). CIDIQ analyses previously confirmed that pDNA was taken up by almost all of the cells [14], whereas the nuclear delivery of pDNA was only detected in less than 30% of the cells. We first examined the relationship between nuclear delivery and transgene expression by the dual imaging of nuclear pDNA and marker gene expression.

To establish a dual imaging of nuclear delivery and transgene expression, unlabeled pDNA along with rhodamine-labeled pDNA (1:1 molecular ratio) was condensed together with LipofectAMINE PLUS, since chemical labeling of pDNA with rhodamine reduces availability as the template in the transcription. In the present study, HeLa cells were observed at 3 hours after the transfection, since prolonged incubation results in the disappearance of pDNA clusters presumably because of the diffusion of pDNA. When the green fluorescence protein (GFP) was used as a marker gene, the fluorescence signal was under the detection limit within a short incubation time, since one GFP protein corresponds to one fluorescence unit. To amplify the information on transgene expression as a fluorescence signal, LacZ was adopted as a marker gene. In this case, the expression of one LacZ protein can be converted to a multiple fluorescence signal via its catalytic activity with respect to the cleavage of phenylethyl β-D-1-thiogalactoside into the fluorescence probe. Typical images for the nuclear pDNA (indicated as arrowheads) and the expression of LacZ at 3 hours post-transfection are shown in Figure 1A. The nuclear co-localization of pDNA was detected in a portion of the cells as indicated by the arrow.

In contrast, the fluorescence signal for lacZ expression was equally diffused in the intracellular space.

The efficiencies of nuclear transfer and transcription were quantified using 204 randomly selected cells, and are summarized in Table 1. Nuclear pDNA was observed in only 46 cells (22.5%). These data suggest that the heterogeneous efficiency of the nuclear delivery of pDNA is one of the reasons for heterogeneous gene expression. In almost all of the nuclear pDNA-negative cells LacZ activity was negative, suggesting that the intracellular trafficking of the rhodamine-labeled pDNA reflected that of the unlabeled pDNA well.

If heterogeneous transgene expression were to be attributed only to the nuclear delivery process, LacZ expression should have been detected in all of the nuclear pDNA-positive cells. However, dual imaging showed that LacZ activity was detected only in 15 cells (32.6%) out of 46 nuclear pDNA-positive cells. Furthermore, when LacZ intensity was plotted against the S(nuc) value, which represents the amount of nuclear pDNA [14], a positive correlation was not observed (Figure 1B). On the contrary, an inversed relationship was found (see Discussion). These data indicate that the intranuclear transcription efficiency, after nuclear entry, is also a key factor in the heterogeneity.

Some of the LacZ-positive cells appear to exist as couplets, suggesting that transgene expression is highly related to the cell cycle (Figure 1A). These data prompted us to gain a better understanding of the cell cycle-dependency of nuclear delivery of pDNA and intranuclear transcription.

Assessment of the cell cycle status

Cell cycle status after release from G1-arrest was analyzed by FACS analysis.

Histograms of relative propidium iodide fluorescence, representing the amount of genome DNA, versus the number of cells are shown in Figure 2. Prior to the removal of hydroxyurea, approximately 80% of the cells were enriched at the G1 phase. By 4.5-6 hours, the cells had resumed their progression and the peak for the cell populations began to shift (early S phase). By 9 hours, the cells further progressed in cell cycle and a significant portion began to possess double fluorescence (late S phase). By 12 hours, approximately 90% of the cells had progressed through the S phase and were in the G2/M phase. Within 15 hours, approximately 15% of the cells had undergone mitotic division and had progressed to the G1 phase of the subsequent cell cycle.

Quantitative comparison of cellular uptake and nuclear delivery of pDNA transfected at various cell cycle status.

To assess the relationship between cell cycle status and the nuclear delivery of pDNA, the unlabeled pDNA and rhodamine-labeled pDNA were transfected to the synchronized cells at various cell cycle phases, as illustrated in Figure 3. The time when the hydroxyurea-including media was changed to the culture media is denoted as time 0 in the present study. Transfection was started at -1.5 hour, 1.5 hour, 4.5 hour, 7.5 hour, 10.5 hour, respectively, and then observed after 3 hour. Respective results were represented against the middle time (e.g. 0 hr, 3 hr, 6 hr, 9 hr and 12 hr, respectively). Typical images are shown in Figure 4. Except for the transfection at the early S phase (6 hr), cellular uptake was clearly observed in most of the cells regardless of cell cycle. Surprisingly, in contrast to the currently accepted hypothesis, the nuclear delivery of pDNA (indicated at arrowhead) was observed even in the transfection at G1 (0 hr and 3 hr), late S phase (9 hr) and G2/M phase (12 hr). These images suggest that pDNA enters the nucleus even when the nuclear membrane is intact.

Cellular and nuclear uptakes of pDNA were quantified in terms of pixel areas of cluster (S(tot) and S(nuc), respectively) by CIDIQ in individual 30 cells after transfection at various cell cycle phases (Figure 5). It was previously demonstrated that 30 cells are sufficient to lead a general conclusion from the statistical point of view. Whereas a temporal decrease was found for cellular uptake (S(tot)) at the early S phase (6 hour), variations of S(tot) values were quite comparable in other cell cycle phases (Figure 5A). As a result of poor cellular uptake, the nuclear delivery of pDNA was also diminished at the early S phase (6 hour). Concerning the other phases, it is noteworthy that significant amount of pDNA were delivered to the nucleus even when cells were transfected at the G1 phase (0 hour and 3 hour), which is far from the mitotic events. Especially at 3 hour, the variation of S(nuc) values was not significantly different compared with that of the late S phase (9 hour), the G2/M phase (12 hour) and non-synchronized controls. These data lead to the unexpected conclusion that the cell cycle is not a determining factor in heterogeneous nuclear transfer efficiency. When the efficiency of nuclear delivery at various cell cycle phases was compared in terms of the number of nuclear pDNA-positive cells to that of totally analyzed cells (Nuc(+)/total), this conclusion also holds true; Nuc(+)/total values were also comparable through every cell cycle (Figure 6: open circles).

Quantitative comparison of intranuclear transcription efficiency transfected at various cell cycle phases

The fraction of LacZ-positive cells of the total 200 cells analyzed (Exp(+)/total), were evaluated 3 hour after transfection at various cell cycle phases (Figure 6: crosses). Whereas transfection at the G1 phase (0 hour and 3 hour) to the early S phase (6 hour) rarely resulted in LacZ expression, the Exp(+)/total values were gradually increased

when transfected after the late S phase (9 hour). When transfected at the G2/M phase (12 hour), the corresponding values reached 20%. Thus, transgene expression efficiency was highly dependent on the cell cycle, and the expression was 'turned on' when transfected after the late S phase. Since the nuclear transfer efficiency was independent of the cell cycle except for the early S phase as described above, this cell cycle-dependent expression was likely to be due to cell cycle-dependent transcription.

The efficiency of intranuclear transcription transfected at various cell cycle phases are represented as the fraction of LacZ-positive cells to the nuclear pDNA-positive cells (Exp(+)/Nuc(+)). As indicated by the closed circles in Figure 6, the Exp(+)/Nuc(+) values at the G1 to the early S phases (0 hour and 3 hour) remain less than 6%. Importantly, the corresponding values were sharply increased to 40% at the late S phase (9 hour) and 68% at the G2/M phase (12 hour). These results indicate that transgene transcription was highly dependent on the cell cycle and increased after the late S phase. Thus, transgene transcription was promoted by an unknown intranuclear factor which was dependent on the cell cycle.

Effect of cell cycle on the intrinsic activity of transcriptional factors for CMV promoter

The cell cycle-dependent transgene transcription might be due to factors affecting transcription from the CMV promoter. The intrinsic activities of endogenous transcription factors associated with the CMV promoter at various cell cycle phases were compared by means of luciferase activity of stable transfectants, expressing CMV-driven luciferase-encoding pDNA (pcDNA3.1-Luc). As shown in Figure 7, the stable transfectant exhibited comparable luciferase activity in all phases. Considering the short half-life of luciferase protein in cells (approximately 2~3 h) [27-29], the intrinsic activity

of transcription factors does not appear to be affected by the cell cycle.

Discussion

Heterogeneous transgene expression is a severe disadvantage for the use of artificial vectors, such as lipoplexes. The fact that the cellular uptake of pDNA was observed in a majority of the cells[14, 1, 30] after transfection, suggests that cellular uptake is not likely to be responsible for the heterogeneity. In addition, a recent CIDIQ analysis indicated the efficient cytoplasmic distribution in the majority of the cells[14]. Thus, it is unlikely that the efficiency of endosomal escape is dominant factor in heterogeneous transgene expression, neither. In contrast, the nuclear delivery of pDNA was only detected in less than 30% of cells, Furthermore, a quantitative comparison of intracellular disposition of adenovirus and LipofectAMINE PLUS, a model vector of viral and artificial vectors, respectively unexpectedly revealed that three order of magnitude more potent transfection activity in adenovirus principally arises from intranuclear events, and not from intracellular trafficking towards the nucleus [31]. Therefore, it is highly possible that pharmacodynamics (i.e. transcription) may also contribute to heterogeneous expression. Therefore, we focused on the mechanism responsible for the heterogeneity from the point of view of nuclear transfer and intranuclear transcription. In the present study, a dual imaging system for nuclear delivery and transgene expression (LacZ) was established to distinguish the contribution of heterogeneities between nuclear delivery of pDNA and intranuclear transcription to overall heterogeneity in transgene expression. Since it is likely that a multitude number of pDNAs share their intracellular fate together within 3 hour after transfection, mixture of rhodamine-labeled pDNA and unlabeled pDNA was used in transfection so as to detect the nuclear delivery and transgene expression, respectively[14].

Previous studies showed that transgene expression by lipofection was closely related to

the proliferation activity [32, 33, 2]. Further studies have concluded that transgene expression is sharply enhanced when cells progress through the M phase[5, 6, 10, 8, 9]. This is also supported by our results in Figure 1, and Figure 6 (crosses) showing that some of the LacZ-positive cells are present in a mother-daughter pattern, and that the Exp(+)/Total value was enhanced when transfected close to the M-phase, respectively. Then, it has been considered that the heterogeneity of transgene expression is derived from variations in the cell cycle status in cell populations. To investigate the relationship between cell-cycle and nuclear transfer efficiency or intranuclear transcription efficiency, lipoplex was transfected to synchronized cells at various phases, and the nuclear delivery of pDNA and LacZ expression was then dually visualized. In the present study, we performed dual imaging at 3 h post-transfection based on two aspects. One is from a technical point of view. After the long incubation, nuclear pDNA clusters disappear presumably because the pDNA may have diffused. Therefore, the nuclear delivery of pDNA cannot be evalulated in the case of prolonged incubation. The other is from a practical point of view. When GFP was used as a marker gene, it is possible to evaluate transgene expression after incubation for a longer period of time (i.e. 24 h). In fact, we confirmed that GFP expression efficiency was also increased when exogenous pDNA was introduced to the cells at the S to G_2/M phase (see supplemental figure 1) as demonstrated previously [6]. However, in this case, it is difficult to clarify in which phase pDNA enters the cells, and when transcription is activated. To address this issue, it is advantageous to investigate nuclear transport and transgene expression after a minimum incubation period. Furthermore, analysis after a short incubation can minimize the effect of DNA degradation. To the best of our knowledge, there is no precedent in the literature where cell cycle-dependent transfection efficiency was evaluated within such a short period (3

h). Although 3 h may be insufficient for nuclear decondensation to be complete, the obtained results were consistent with that obtained using longer transfection times (24 h) as represented in supplemental figure 1. Therefore, the mechanism of heterogeneity can be clarified by using short time incubation (3 h), and is likely to be applicable to that observed in commonly used incubation times (i.e.24 h).

Concerning cell synchronization, various methods (i.e. double tymidine block (G1/S phase) [7, 9], aphydicoline (S phase) [7, 8, 34] and nocodazol/pacritaxel (M phase) [34]) have been used in previous studies. To simply interpret the obtained results, it is convenient to use synchronized cell populations starting from, and turning back to the G_1 phase via the G_2/M phase. Therefore, in the present study, hydroxyurea was used to synchronize the cell cycle to the G_1 phase, and cell cycle arrest was then released by changing the medium to hydroxyurea-free medium to obtain cell populations that are synchronized at various phases. Although hydroxyurea have a side effect to elongate the S phase by arresting DNA replication [35], the time-dependent proceeding of cell cycle was confirmed by flow cytometry after the release from cell cycle arrest (Figure 2). Furthermore, it has been reported that hydroxyurea treatment induces transcription factors such as p53 [36], which alters the transcription activity of certain types of proteins [37]. However, hydroxyurea had little effect on the expression level of GL3, stably expressed in HeLa cells under the regulation of the CMV promoter (Figure 7). Therefore, these side effects may not be a severe problem, at least in the present experiment. Collectively, these data indicated that hydroxyurea is useful for preparing synchronized cell populations for the investigation of cell-cycle dependent nuclear transfer and nuclear transcription.

Concerning nuclear delivery, the fraction of nuclear pDNA-positive cells was limited to

22.5% of the cells analyzed (Figure 1A and Table 1) in unsynchronized cells. This suggests that cell-to-cell difference in nuclear delivery is one of the reasons for heterogeneous transgene expression. Many investigators have speculated that M-phase dependent nuclear import during the breakdown of the nuclear membrane was the main reason for heterogeneous nuclear transfer, based on data showing improved transfection efficiency during mitosis. As shown in Figure 2, approximately 20% of the cells were likely to be in the S or G_2/M phases throughout the experiment. Therefore, a certain percentage of nuclear transfer might be achieved when cells undergo mitosis. However, it sould be noted that nuclear transfer efficiency in terms of Nuc(+)/Total (%) was not enhanced in the G2/M phases (Figure 6; open circle) indicating that the mitotic event alone cannot explain the mechanism for the nuclear transfer of pDNA. This is supported by the fact that nuclear pDNA was observed in singlet cells in the G1~late S phases (Figure 4). Furthermore, the pixel areas of pDNA in nucleus (S(nuc)) along with that in whole cell (S(tot)) were comparable regardless of the timing of transfection (Figure 5) although those values were temporally decreased when transfected around early S phase (6 hour). Considering that cells in the S phase constitute only 10% of the unsynchronized control cell population (data not shown), the contribution of poor cellular uptake and nuclear delivery when transfected at the early S phase would be inefficient to explain the overall heterogeneity of transgene expression. Considering the observed size of the pDNA clusters (approximately 1 μm: Figure 4), it is likely that pDNA enters the a nucleus via nuclear pore complex (NPC)-independent pathway since the NPC cannot accept macromolecules with a diameter of >39 nm[38]. We proposed a fusion hypothesis to explain the nuclear delivery of pDNA with LFN[39]. This fusion mechanism is also supported by electron micrographs, which indicate a morphological change in the nuclear

membrane after transfection with cationic liposomes[40]. Taking these findings into consideration, pDNA transfected with LFN could pass through the nuclear membrane even in the non-mitotic phase presumably by a fusion mechanism.

However, the mechanism of the cell-cycle independent nuclear delivery efficiency remains unclear. It may be accounted for by the intracellular form of pDNA in the cell, and the driving force to access the nucleus. Majority of the pDNA was detected as clustered forms, but not as diffused forms (Figures 1A and 4). In addition, the expression of LacZ was barely detectable in nuclear pDNA-negative cells, indicating that little, if any, un-clustered pDNA was delivered into the nucleus (Table 1). These data suggest that large numbers of pDNA molecules behaved as limited numbers of aggregates in the cells, but not as mono-dispersed forms. Furthermore, it is possible that the driving force for the lipoplex to gain access to the nucleus from the cytoplasm is electrostatic interactions between the positively charged lipoplex and negatively charged lipids on the nuclear membrane[41]. Therefore, the nuclear delivery of the lipoplex may be interrupted by non-specific binding with various intracellular organelles such as mitochondria, which also contain high levels of negatively charged lipids[41]. As a result, only a small fraction of the aggregates would be able to reach the nucleus. In this sense, heterogeneous nuclear delivery may be subject to the theory of probability. This hypothesis is also supported by the mechanism concerning the intracellular trafficking of adenovirus, which exhibits non-heterogeneous transgene expression. It exists as mono-dispersed form in the cell, and utilizes an active microtubule network, which specifically directs it to the nucleus[42, 43]. To overcome heterogeneous nuclear delivery, intracellular delivery of pDNA as dispersed particles, along with a specific nuclear targeting system may be essential.

From a pharmacodynamic point of view, only 32.6% of the nuclear pDNA-positive

cells exhibited transgene expression in non-synchronized cells (Table 1). As a result, cell-to-cell difference in intranuclear transcription is also responsible for heterogeneous transgene expression. An analysis of synchronized cells further indicated that intranuclear transcription was drastically affected by the cell cycle (Figure 6: closed circle). The Exp(+)/Nuc(+) values were drastically enhanced when transfected at the late S and G2/M phases, but severely restricted during the G1 to early S phases. This finding raises the question of whether intranuclear events during the S to M phases or the cell division contributed to the enhanced transgene expression. At the G2/M phase (12 hour), when the Exp(+)/Total and Exp(+)/Nuc(+) values were maximal, the population of G1 phase was limited to less than 1% (Figure 2). This suggests that intranuclear transcription is likely linked with events during the S to M phases, but not with the division of cells. In contrast, the expression of luciferase, driven by the CMV promoter in stably expressing cells, was comparable regardless of the cell cycle (Figure 7), suggesting that the function of intrinsic transcription factors for the CMV promoter are independent of cell cycle. Thus, the cell cycle dependent variation in transcription seems to be derived from the intranuclear ‘condition’ of exogenous pDNA. Considering previous results showing that transgene expression after the nuclear microinjection of pDNA is severely inhibited when pDNA is injected as a lipoplex [44, 45, 30], release of pDNA from the cationic lipids is essential to allow the transcription factors to access to the promoter. We assume that proteins that are able to bind to DNA in the nucleus play important roles. During the S phase, basic proteins such as histones are synthesized in harmony with DNA synthesis [46, 47]. It has been reported that amounts of histone mRNAs increase to 15-fold during the S phase [46, 47]. The nuclear accumulation of histones may induce the decondensation of pDNA by replacing the counterpart from cationic liposomes to basic

proteins as histone itself, and presumably forming a nucleosome structure, which is advantageous for efficient transcription. As shown in Figure 1B, the S(nuc) values for transgene expression-positive cells (represented as open symbols, on average 146.5) were significantly lower than those for transgene expression-negative cells (represented as closed symbols, on average 360.6). This lower S(nuc) values were derived from smaller pixel areas of an individual cluster but not from smaller number of the clusters (data not shown). It can be easily imagined that cationic lipids in the huge complex with pDNA would be replaced with difficulty by basic proteins. These data also support that the replacement of the pDNA condenser from cationic liposomes to histones is a key factor of transgene transcription.

Finally, it should be noted that the mechanism of heterogeneity may be different between lipoplexes and polyplexes. The discussion of the mechanism of nuclear transfer via fusion cannot be applicable to a polyplex. Furthermore, a previous nuclear microinjection study indicated that the transgene expression microinjection pDNA was severely impaired when pDNA was injected with cationic liposomes, whereas a less inhibitory effect was found for a polyplex (e.g. polyethyleneimine) [44]. Therefore, the proposed mechanism for enhancement of intranuclear transcription (e.g. replacement of counterparts to histons) may be more applicable to lipoplex systems compared to polyplex systems than to polyplex systems. The contribution of nuclear transcription to heterogeneity in polyplex-mediated transfection remains to be investigated.

The mechanism responsible for heterogeneity in lipoplex-mediated transfection was investigated from the point of view of intracellular pharmacokinetics and intranuclear pharmacodynamics. Concerning the pharmacokinetics, our previous CIDIQ analysis showed that nuclear transfer, but not cellular uptake or endosomal escape was closely

related to the heterogeneity of transgene expression. Further imaging of the nuclear delivery of pDNA to synchronized cells unexpectedly revealed that nuclear transfer efficiency is independent of the cell cycle, which fact is antithesis of the general consideration that the nuclear import of pDNA is enhanced during cell division when the nuclear membrane structure is perturbed. In contrast, dual imaging of the nuclear delivery of pDNA and transgene expression indicated that intranuclear transcription of pDNA transfected by LFN is highly dependent on the cell cycle: it is drastically enhanced in the late S to G2/M phase. Therefore, we propose a novel hypothesis that cell-cycle dependent transgene expression is mainly due to intranuclear transcription initiated by replacing a counterpart of the pDNA from cationic lipids with basic proteins as histones. This is a first demonstration, which shows that cell-cycle dependent intranuclear transcription is a key factor for the overall heterogeneity of transgene expression.

Acknowledgements

This work was supported in part by Grants-in-Aid for Scientific Research on Priority Areas from the Japan Society for the Promotion of Science, and by Grant-in-Aid for Young Scientists (B) from the Ministry of Education, Culture, Sports, Science and Technology of Japan, and by Grants-in-Aid for Scientific Research on Priority Areas from the Japan Society for the Promotion of Science. We also thank Dr. Milton S. Feather for helpful advice in the use of English in this manuscript.

References

1. Tseng, W.C., Haselton, F.R. and Giorgio, T.D.Transfection by cationic liposomes using simultaneous single cell measurements of plasmid delivery and transgene expression. *J Biol Chem*.1997; **272**: 25641-25647.
2. Wilke, M., Fortunati, E., van den Broek, M., et al.Efficacy of a peptide-based gene delivery system depends on mitotic activity. *Gene Ther*.1996; **3**: 1133-1142.
3. Newgard, C.B., Hwang, P.K. and Fletterick, R.J.The family of glycogen phosphorylases: structure and function. *Crit Rev Biochem Mol Biol*.1989; **24**: 69-99.
4. Scholl, B., Gervaz, P., Martinet, O., et al.Adenovirus-mediated gene transfer into selected liver segments using a vascular exclusion technique. *Eur Surg Res*.2001; **33**: 348-354.
5. Brunner, S., Furtbauer, E., Sauer, T., et al.Overcoming the nuclear barrier: cell cycle independent nonviral gene transfer with linear polyethylenimine or electroporation. *Mol Ther*.2002; **5**: 80-86.
6. Brunner, S., Sauer, T., Carotta, S., et al.Cell cycle dependence of gene transfer by lipoplex, polyplex and recombinant adenovirus. *Gene Ther*.2000; **7**: 401-407.
7. Escriou, V., Carriere, M., Bussone, F., et al.Critical assessment of the nuclear import of plasmid during cationic lipid-mediated gene transfer. *J Gene Med*.2001; **3**: 179-187.
8. Mortimer, I., Tam, P., MacLachlan, I., et al.Cationic lipid-mediated transfection of cells in culture requires mitotic activity. *Gene Ther*.1999; **6**: 403-411.
9. Tseng, W.C., Haselton, F.R. and Giorgio, T.D.Mitosis enhances transgene expression of plasmid delivered by cationic liposomes. *Biochim Biophys Acta*.1999; **1445**: 53-64.
10. James, M.B. and Giorgio, T.D.Nuclear-associated plasmid, but not cell-associated plasmid, is correlated with transgene expression in cultured mammalian cells. *Mol Ther*.2000; **1**: 339-346.
11. Greber, U.F., Suomalainen, M., Stidwill, R.P., et al.The role of the nuclear pore complex in adenovirus DNA entry. *Embo J*.1997; **16**: 5998-6007.
12. Greber, U.F., Willetts, M., Webster, P., et al.Stepwise dismantling of adenovirus 2 during entry into cells. *Cell*.1993; **75**: 477-486.
13. Trotman, L.C., Mosberger, N., Fornerod, M., et al.Import of adenovirus DNA involves the nuclear pore complex receptor CAN/Nup214 and histone H1. *Nat Cell Biol*.2001; **3**: 1092-1100.
14. Akita, H., Ito, R., Khalil, I.A., et al.Quantitative three-dimensional analysis of the intracellular trafficking of plasmid DNA transfected by a nonviral gene delivery system using confocal laser scanning microscopy. *Mol Ther*.2004; **9**: 443-451.
15. Nakao, M.Epigenetics: interaction of DNA methylation and chromatin. *Gene*.2001; **278**: 25-31.
16. Umlauf, D., Goto, Y. and Feil, R.Site-specific analysis of histone methylation and acetylation. *Methods Mol Biol*.2004; **287**: 99-120.
17. Brooks, A.R., Harkins, R.N., Wang, P., et al.Transcriptional silencing is associated with extensive methylation of the CMV promoter following adenoviral gene delivery to muscle. *J Gene Med*.2004; **6**: 395-404.
18. Singal, R., Ferris, R., Little, J.A., et al.Methylation of the minimal promoter of

an embryonic globin gene silences transcription in primary erythroid cells. *Proc Natl Acad Sci U S A*.1997; **94**: 13724-13729.
19. Carmo-Fonseca, M.The contribution of nuclear compartmentalization to gene regulation. *Cell*.2002; **108**: 513-521.
20. Gasser, S.M.Visualizing chromatin dynamics in interphase nuclei. *Science*.2002; **296**: 1412-1416.
21. Stein, G.S., Zaidi, S.K., Braastad, C.D., et al.Functional architecture of the nucleus: organizing the regulatory machinery for gene expression, replication and repair. *Trends Cell Biol*.2003; **13**: 584-592.
22. Ochiai, H., Harashima, H. and Kamiya, H.Intranuclear disposition of exogenous DNA in vivo: silencing, methylation and fragmentation. *FEBS Lett*.2006; **580**: 918-922.
23. Ochiai, H., Harashima, H. and Kamiya, H.Silencing of exogenous DNA in cultured cells. *Biol Pharm Bull*.2006; **29**: 1294-1296.
24. Sasaki, K., Murakami, T., Kawasaki, M., et al.The cell cycle associated change of the Ki-67 reactive nuclear antigen expression. *J Cell Physiol*.1987; **133**: 579-584.
25. Wersto, R.P., Chrest, F.J., Leary, J.F., et al.Doublet discrimination in DNA cell-cycle analysis. *Cytometry*.2001; **46**: 296-306.
26. Ito, K., Suzuki, H., Hirohashi, T., et al.Functional analysis of a canalicular multispecific organic anion transporter cloned from rat liver. *J Biol Chem*.1998; **273**: 1684-1688.
27. Leclerc, G.M., Boockfor, F.R., Faught, W.J., et al.Development of a destabilized firefly luciferase enzyme for measurement of gene expression. *Biotechniques*.2000; **29**: 590-591, 594-596, 598 passim.
28. Thompson, J.F., Hayes, L.S. and Lloyd, D.B.Modulation of firefly luciferase stability and impact on studies of gene regulation. *Gene*.1991; **103**: 171-177.
29. Yamada, Y., Kamiya, H. and Harashima, H.Kinetic analysis of protein production after DNA transfection. *Int J Pharm*.2005; **299**: 34-40.
30. Zabner, J., Fasbender, A.J., Moninger, T., et al.Cellular and molecular barriers to gene transfer by a cationic lipid. *J Biol Chem*.1995; **270**: 18997-19007.
31. Hama, S., Akita, H., Ito, R., et al.Quantitative comparison of intracellular trafficking and nuclear transcription between adenoviral and lipoplex systems. *Mol Ther*.2006; **13**: 786-794.
32. Fasbender, A., Zabner, J., Zeiher, B.G., et al.A low rate of cell proliferation and reduced DNA uptake limit cationic lipid-mediated gene transfer to primary cultures of ciliated human airway epithelia. *Gene Ther*.1997; **4**: 1173-1180.
33. Jiang, C., O'Connor, S.P., Fang, S.L., et al.Efficiency of cationic lipid-mediated transfection of polarized and differentiated airway epithelial cells in vitro and in vivo. *Hum Gene Ther*.1998; **9**: 1531-1542.
34. Seidman, M.A., Hogan, S.M., Wendland, R.L., et al.Variation in adenovirus receptor expression and adenovirus vector-mediated transgene expression at defined stages of the cell cycle. *Mol Ther*.2001; **4**: 13-21.
35. Koc, A., Wheeler, L.J., Mathews, C.K., et al.Hydroxyurea arrests DNA replication by a mechanism that preserves basal dNTP pools. *J Biol Chem*.2004; **279**: 223-230.
36. Kumar, S., Dodson, G.E., Trinh, A., et al.ATR activation necessary but not sufficient for p53 induction and apoptosis in hydroxyurea-hypersensitive myeloid

leukemia cells. *Cell Cycle*.2005; **4**: 1667-1674.
37. Fingerman, I.M. and Briggs, S.D.p53-mediated transcriptional activation: from test tube to cell. *Cell*.2004; **117**: 690-691.
38. Pante, N. and Kann, M.Nuclear pore complex is able to transport macromolecules with diameters of about 39 nm. *Mol Biol Cell*.2002; **13**: 425-434.
39. Kamiya, H., Fujimura, Y., Matsuoka, I., et al.Visualization of intracellular trafficking of exogenous DNA delivered by cationic liposomes. *Biochem Biophys Res Commun*.2002; **298**: 591-597.
40. Friend, D.S., Papahadjopoulos, D. and Debs, R.J.Endocytosis and intracellular processing accompanying transfection mediated by cationic liposomes. *Biochim Biophys Acta*.1996; **1278**: 41-50.
41. Daum, G.Lipids of mitochondria. *Biochim Biophys Acta*.1985; **822**: 1-42.
42. Suomalainen, M., Nakano, M.Y., Boucke, K., et al.Adenovirus-activated PKA and p38/MAPK pathways boost microtubule-mediated nuclear targeting of virus. *Embo J*.2001; **20**: 1310-1319.
43. Suomalainen, M., Nakano, M.Y., Keller, S., et al.Microtubule-dependent plus- and minus end-directed motilities are competing processes for nuclear targeting of adenovirus. *J Cell Biol*.1999; **144**: 657-672.
44. Pollard, H., Remy, J.S., Loussouarn, G., et al.Polyethylenimine but not cationic lipids promotes transgene delivery to the nucleus in mammalian cells. *J Biol Chem*.1998; **273**: 7507-7511.
45. Tachibana, R., Harashima, H., Ishida, T., et al.Effect of cationic liposomes in an in vitro transcription and translation system. *Biol Pharm Bull*.2002; **25**: 529-531.
46. Heintz, N., Sive, H.L. and Roeder, R.G.Regulation of human histone gene expression: kinetics of accumulation and changes in the rate of synthesis and in the half-lives of individual histone mRNAs during the HeLa cell cycle. *Mol Cell Biol*.1983; **3**: 539-550.
47. Sittman, D.B., Graves, R.A. and Marzluff, W.F.Histone mRNA concentrations are regulated at the level of transcription and mRNA degradation. *Proc Natl Acad Sci U S A*.1983; **80**: 1849-1853.

Figure legends

Figure 1

Dual imaging of nuclear delivery of pDNA and LacZ expression.

A. A 1:1 mixture of LacZ-encoding pDNA and a rhodamine-labeled one was transfected to HeLa cells by LFN. At 3 hour post-transfection, the nucleus was stained by incubation with Hoechst 33342 (Blue). Nuclear transferred pDNA was detected as red clusters as indicated by an arrowhead. Transgene expression was further visualized with an *in vivo* lacZ β-Galactosidase Detection Kit (Green). B. Relationship between transgene expression of LacZ and the total pixels corresponding to nuclear clusters of pDNA: S(nuc). The expression of LacZ was photographically quantified in terms of the mean fluorescence intensity of phenylethyl β-D-1-thiogalactoside, which is fluorescently activated in response of the expression level of LacZ. Cells with fluorescence more than the threshold (200 fluorescence intensity per pixel) were judged as LacZ-expressing cells. This threshold was determined in preliminary transfection experiments using the luciferase gene. Total pixels of nuclear co-localized pDNA clusters: S(nuc) was quantified by means of CIDIQ method. Open circles, LacZ expression-positive cells; closed symbols, LacZ expression-negative cells. $^{**}P<0.01$ between the LacZ expression-positive and -negative groups.

Figure 2

Time profiles for the progress of cell cycle after the release from G1 arrest.

HeLa cells were synchronized to the G1-phase by treatment with hydroxyurea at a concentration of 2 mg/ml for 18 hour. At time 0, the hydroxyurea was removed and replaced with fresh growth media to allow the cells to release from G1 arrest. Histograms

of relative iodide fluorescence versus the number of cells are shown. For each time, the breakdown of the population according to the cell phase is indicated.

Figure 3

Schematic diagram illustrating the time course of the transfection experiments.

HeLa cells were synchronized to the G1-phase by treatment with hydroxyurea. At time 0, hydroxyurea was removed and replaced incubate with fresh growth media for the release from G1 arrest. At –1.5 hour, 1.5 hour, 4.5 hour, 7.5 hour and 10.5 hour, mixture of rhodamine-labeled and unlabeled LacZ-pDNA was transfected. After 3hour incubation, the nuclear delivery of pDNA and transgene expression was visualized as described in the material and methods section. The results are represented against the middle time of incubation (i.e. 0 hour, 3 hour, 6 hour, 9 hour and 12 hour).

Figure 4

Confocal images for the nuclear entry of pDNA.

At 3 hour post-transfection with rhodamine-labeled pDNA at various cell cycle phases, the nucleus was stained with Hoechst 33342 and confocal images were captured. Typical images, when transfection was performed at 0 hour, 3 hour, 6 hour, 9 hour and 12 hour after release from G1 arrest were indicated as A-E. Red and blue signals represent clusters of pDNA and the nucleus, respectively.

Figure 5

Quantitative comparison of the cellular uptake and nuclear transfer of pDNA transfected at various cell cycle phases.

After transfection for 3 hour at various cell cycle status as illustrated in Figure 3, the cellular uptake (A) and nuclear transfer (B) of pDNA in terms of S(tot) and S(nuc), respectively were quantified as described in the material and methods section. Each bar represents the mean values and standard deviation for 30 analyzed cells. The open bar represents the result for unsynchronized control cells. The black bar in B represents mean values of 30 analyzed cells.

Figure 6

Effect of the cell cycle on the nuclear transfer efficiency, transgene expression efficiency and intranuclear transcription efficiency.

After transfection for 3 hour at various cell cycle statuses, the nuclear transfer of pDNA and transgene expression was visualized. The efficiency of transgene expression in terms of the fraction of transgene expression-positive cells to totally analyzed cells (Exp(+)/Total), nuclear transfer efficiency in terms of the fraction of nuclear pDNA-positive cells to the total cells analyzed(Nuc(+)/Total) and intranuclear transcription efficiency in terms of the fraction of transgene expression-positive cells to nuclear pDNA-positive cells (Exp(+)/Nuc(+)) are plotted as crosses, open circle and closed circle, respectively. Data was represented as mean value of typical experiments (n=2).

Figure 7

Effect of the cell cycle on CMV promoter-driven luciferase activity in stably expressed cells.

After the synchronization of stably transfected HeLa cells expressing CMV-driven

luciferase, G1-arrest was released at time 0 hour. At the indicated times, the luciferase activity was measured. Each bar represents the mean value and standard deviation for triplicate experiments. The open bar represents the results for unsynchronized control cells.

Table 1 Quantitative evaluation of the dual imaging of the nuclear delivery of pDNA and LacZ expression [a]

	LacZ expression (+)	LacZ expression (–)	Subtotal
Nuclear transfer (+)	15 [32.6%] [*]	31 [67.4%] [*]	46 [22.5%] [**]
Nuclear transfer (–)	3 [1.2%] [*]	155 [98.8%] [*]	158 [77.5%] [**]
Total			204 [100%]

204 randomly selected HeLa cells were analyzed to count the cells representing the nuclear delivery of pDNA and LacZ expression.

[*] The percentage of LacZ expression-positive or -negative cells of total nuclear pDNA-positive/negative cells.

[**] The percentage of nuclear pDNA-positive or -negative cells to the total cells analyzed.

Figure 1

A

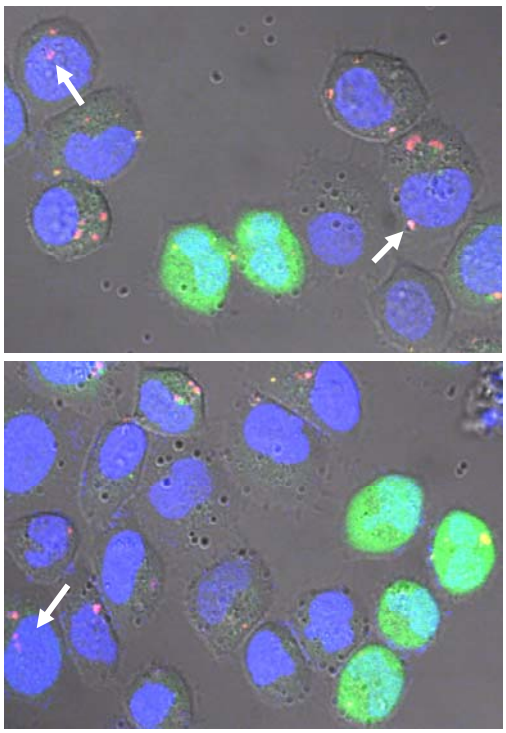

B

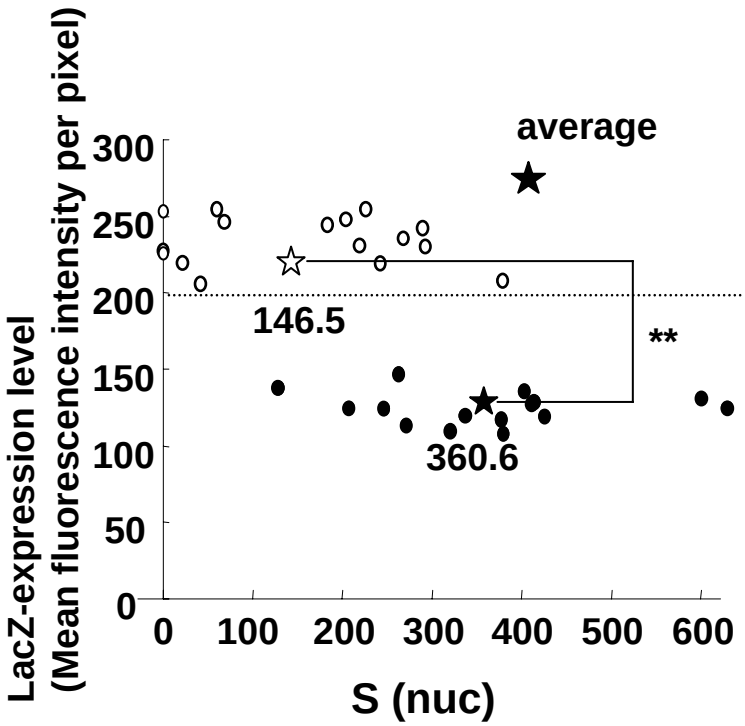
LacZ-expression level
(Mean fluorescence intensity per pixel)
300
250
200
150
100
50
0
average
146.5
360.6
**
0
100
200
300
400
500
600
S (nuc)

Figure 2

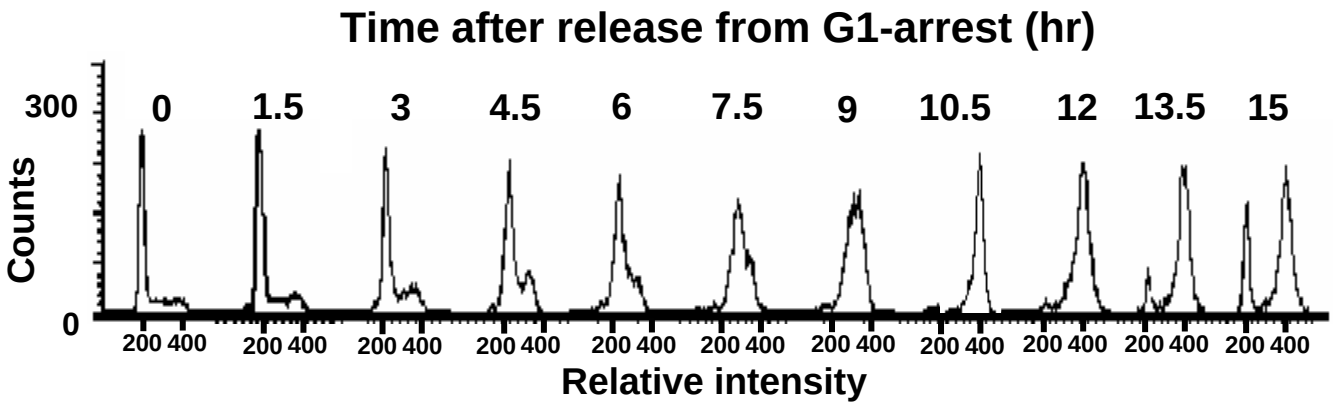

G0/G1	81.1	72.7	23.2	4.1	3.8	2.4	1.6	1.7	1.8	7.6	34.6
S	9.6	11.9	62.5	79.4	78.3	73.9	59.6	41.0	10.0	8.7	6.8
G2/M	9.6	11.3	15.8	16.5	18.5	24.3	39.6	58.7	88.7	93.8	68.8

(%)

Figure 3

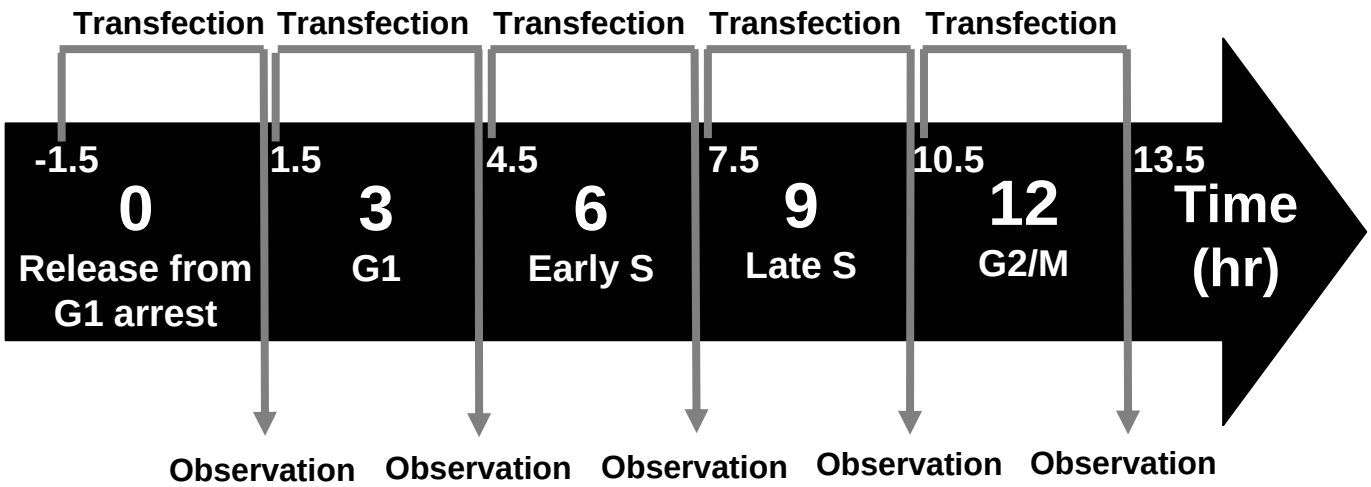
Transfection
Transfection
Transfection
Transfection
Transfection
-1.5
1.5
4.5
7.5
10.5
13.5
0
Release from G1 arrest
3
G1
6
Early S
9
Late S
12
G2/M
Time (hr)
Observation
Observation
Observation
Observation
Observation

Figure 4

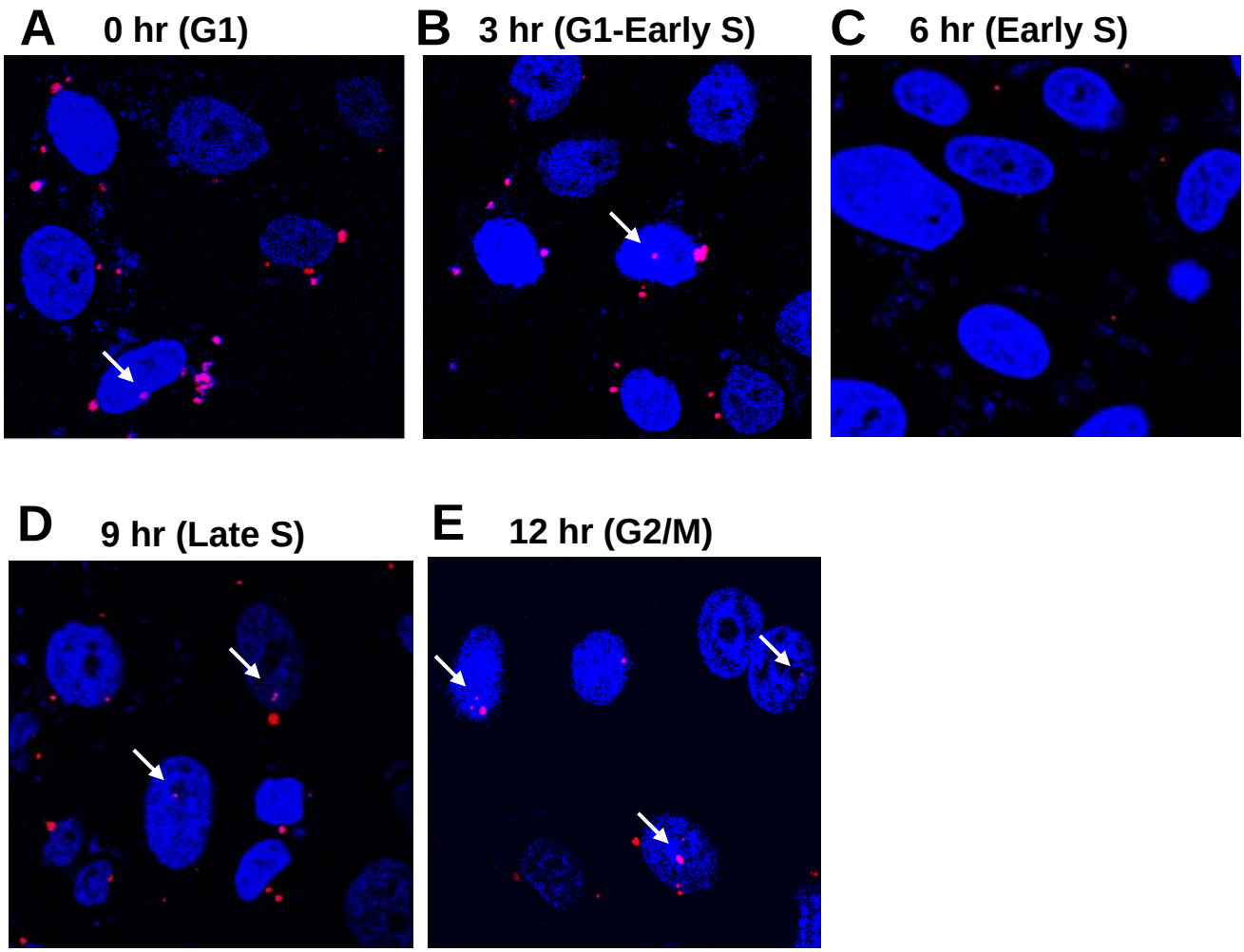

Figure 5

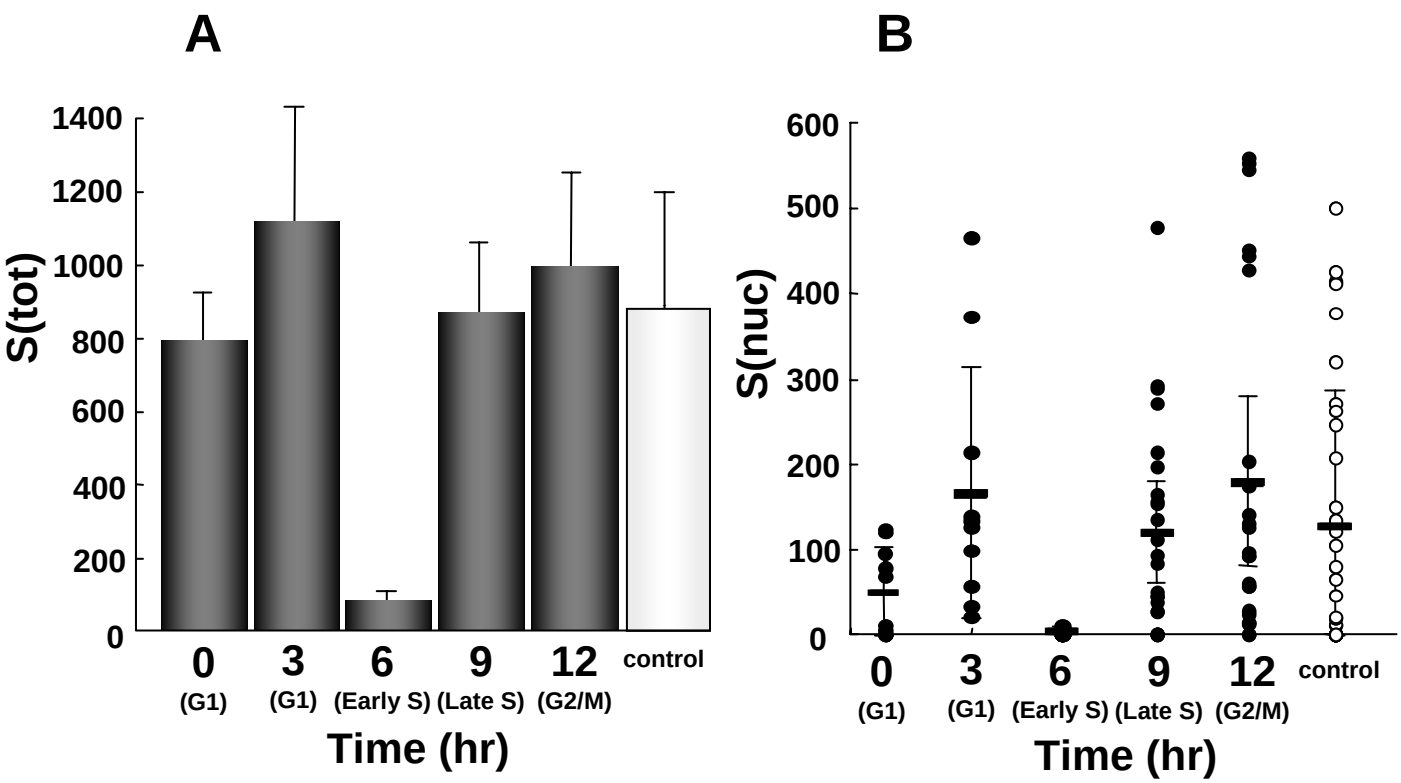
A
B
S(tot)
S(nuc)
1400
1200
1000
800
600
400
200
0
600
500
400
300
200
100
0
0
(G1)
3
(G1)
6
(Early S)
9
(Late S)
12
(G2/M)
control
Time (hr)

Figure 6

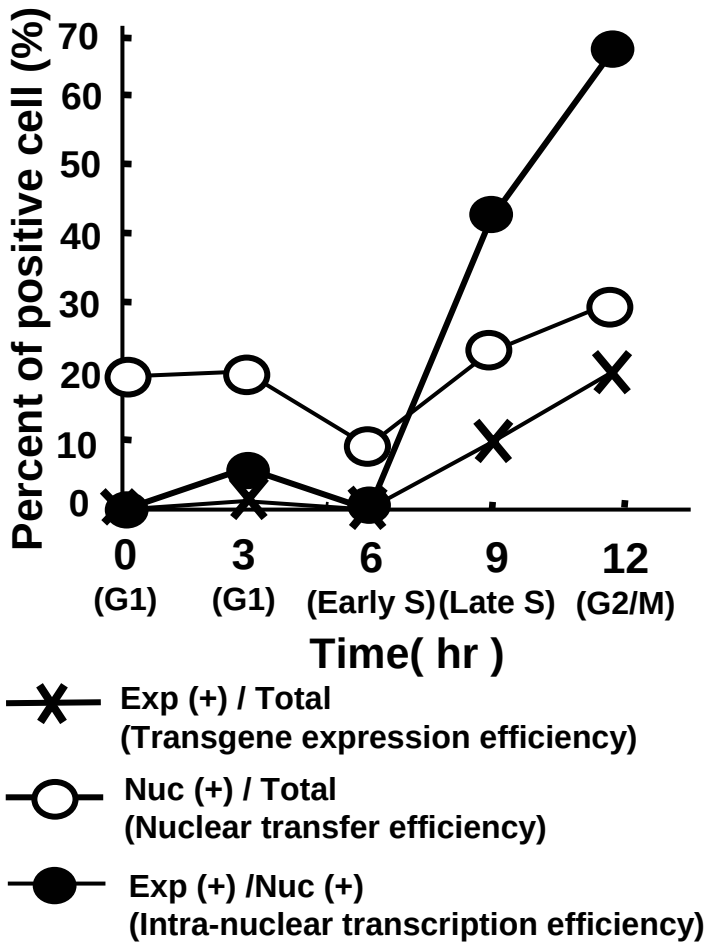
Percent of positive cell (%)
70
60
50
40
30
20
10
0
0
3
6
9
12
(G1)
(G1)
(Early S)
(Late S)
(G2/M)
Time(hr)
Exp (+) / Total
(Transgene expression efficiency)
Nuc (+) / Total
(Nuclear transfer efficiency)
Exp (+) /Nuc (+)
(Intra-nuclear transcription efficiency)

Figure 7

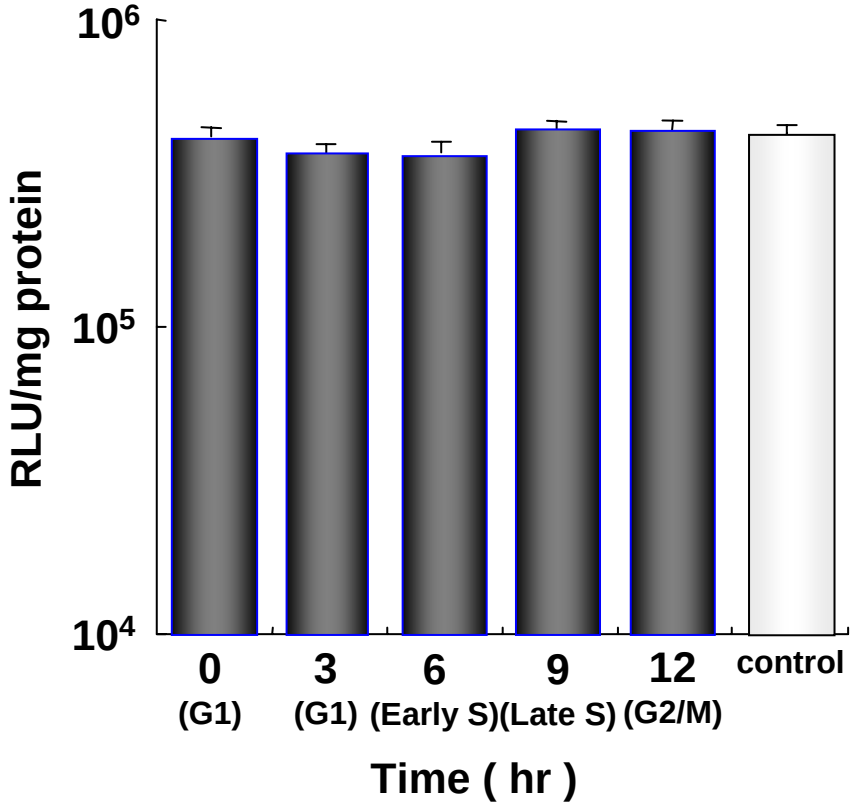
10^6
10^5
10^4
RLU/mg protein
0
(G1)
3
(G1)
6
(Early S)
9
(Late S)
12
(G2/M)
control
Time (hr)